Journal of the European Ceramic Society 17 (1997) 1631–1638

PII: S0955-2219(97)00020-4
0955-2219/97/$17.00 + 0.00

Nucleation and Growth of the Elongated α'-SiAlON

Xu Fang-Fang,[a] Wen Shu-Lin,[a] L.-O. Nordberg[b] & T. Ekstrom[b]

[a]Shanghai Institute of Ceramics, Chinese Academy of Sciences, Shanghai, P. R. China
[b]Department of Inorganic Chemistry, Arrhenius Laboratory, Stockholm University, Stockholm, Sweden

(Received 30 August 1996; accepted 13 January 1997)

Abstract

Nucleation and growth behavior of the elongated α′-SiAlON grains have been studied in α′-SiAlON ceramic with an overall composition $Y_{0.48}Si_{10.00}Al_{2.30}O_{1.17}N_{15.29}$ *prepared by hot-pressing at 1825°C. Transmission electron microscopy (TEM) and high resolution electron microscopy (HREM) have shown that the elongated α′-SiAlON grains always contain an* α-Si_3N_4 *core, implicating heterogeneous nucleation operating in the present system. The growth mode is epitaxial. Selected area diffraction (SAD) and HREM analyses reveal that the crystal structure of the elongated α′-SiAlON has dilated and does not strictly comply with the hexagonal construction, i.e. the c axis tilting by no more than 2° is no longer normal to (001) plane, giving a conclusion that the deformed structure, probably formed by local high stress at high temperatures, changes the chemical bonding conditions especially on (001) plane, leading to faster deposition of atoms on (001) plane than on other planes. Additionally, morphology and growth defects have been studied in this paper.* © *1997 Elsevier Science Limited.*

1 Introduction

Hot-pressing with α-Si_3N_4, AlN, Al_2O_3 and Y_2O_3 as starting powders may form α'-SiAlON, a solid solution with various compositions expressed as $Y_{m/3}Si_{12-(m+n)}Al_{m+n}O_nN_{16-n}$.[1,2] The capacity for incorporating a variety of metal ions into the interstices of the structure affords the possibility of making nitride ceramics of a much lower glass content, leading to a very impressive high-temperature strength.[3–7] But the equiaxed nature of α'-SiAlON grains makes it poor in toughness compared with the β'-SiAlON ceramics which possess a high degree of toughness by self-enhancement with the elongated β'-SiAlON grains.[8–13] So, α'-SiAlON is usually incorporated with second phases such as SiC(w), TiN, $MoSi_2$ or β'-SiAlON, forming the composites to improve the mechanical properties.[14–17] Materials with elongated α'-SiAlON grains have been recently produced in some laboratories. This significant new success will surely broaden the utility of the α'-SiAlON ceramics.

Studies on nucleation and growth of equiaxed α'-SiAlON have been reported before.[18] Heterogeneous nucleation and epitaxial growth mode of large grains often accepted to be the case in many α'-SiAlON containing material. Although the elongated α'-SiAlON grains appear exclusively large, its anisotropic growth habit, regardless of its nature in lacking any special growth direction due to the chemical bonding considerations,[18] implies a special nucleation and growth mechanism.

In *in-situ* work, our first interest is in the relationship between microstructure and mechanical properties of the various amounts of $MoSi_2$-particle reinforced α'-SiAlON composites. When TEM had discovered the elongated grains commonly existing in these series of materials, pure α'-SiAlON with the same composition was then prepared as a reference under the same preparation conditions and during the same process. The fact of the appearance of these elongated grains in pure α'-SiAlON material confused us as we had expected that the second phase ($MoSi_2$ in this work) might have played a role in this special growth habit. Then there must be a definite growth mechanism taking effect independent of second phase.

In the present work, transmission electron microscopy is used to elucidate the microscopic aspects of the nucleation and specific growth behavior of the elongated α'-SiAlON grains.

2 Experimental procedure

Pure α'-SiAlON was prepared from α-Si_3N_4 (UBE, Grade SN10E), AlN(HC Starck, grade A) and Y_2O_3(HC Starck, grade finest) as starting powders mixed by ultrasonic dispersion in water-free isopropanol. The extra oxygen present in the nitrides is accounted for in the formula $(Y_xSi_{12-4.5x}Al_{4.5x}O_{1.5x}N_{16-1.5x})$ x = 0·48 giving the overall composition $Y_{0.48}Si_{10.00}Al_{2.30}O_{1.17}N_{15.29}$. Full densification was achieved by hot-pressing at 1825°C, with a pressure of 35 MPa and a holding time of 1 h.

Specimens for TEM studies were prepared by cutting thin sections from the hot-pressed disc. The thin section was mechanically polished to a thickness of less than 30 μm. Then it was ion milled using the Gatan-600 ion beam thinner at a voltage of 4 kV and an incidence beam angle of 15° until the specimen was perforated. Finally, the ultra-thin plate was sputtered with amorphous carbon to the thickness of about several decades of nanometers.

HREM was performed on a JEM-200CX with an operating voltage of 200 kV using a top entry double-tilt specimen holder. The pure gold was used as the standard sample for TEM calibration in order to give precise values of interplanar distances. Energy dispersive X-ray analysis was performed using an EDS (Link-6498) as accessory to a TEM (JEM2010) with an operating voltage of 200 kV using a side entry double-tilt specimen holder.

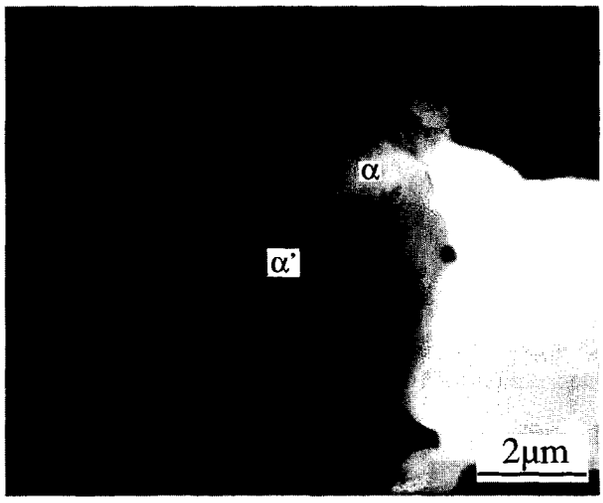

(a)

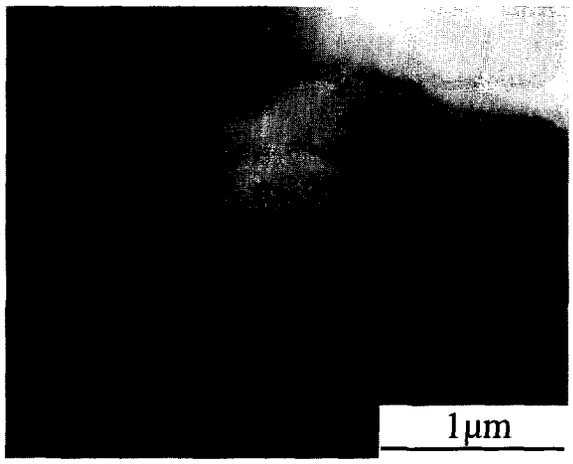

(b)

Fig. 1. A typical microstructure of an elongated α'-SiAlON grain which contains a core with a lighter contrast. A strong contrast at the boundary between the core and the shell indicates the presence of misfit strain fields.

3 Results

3.1 Heterogeneous nucleation and anisotropic growth

Figure 1(a) shows a typical microstructure constituted of an elongated grain surrounded by small equiaxed particles. The normal size of the elongated grains is 9 ~ 12 μm in length and 1.5 ~ 3 μm in width. The long direction of the grain is parallel to [001] and the aspect ratio is up to 5. The [001] growth front appears acicular and the interface along the [210] growth front is unexpectedly wavy rather than flat while sharp interface is often the case for the elongated β' grains.

TEM observation shows that the elongated α' grains, like other larger equiaxed α' grains, always contain a core with a contrast lighter than that of the surrounding shell under bright-field imaging conditions. Figure 1(b) clearly illustrates the misfit dislocations at the boundary between the core and the shell due to the disparity of the lattice parameters between the two phases. Selected area diffraction (SAD) patterns and HREM micrographs (Fig. 2) show that the core and the shell have the same α-Si_3N_4 structure and crystallographic orientation. The interface between the core and the shell is coherent, as revealed by the continuity of the lattice planes across the interface. The measurement of the interplanar distance in the lattice image shown in Fig. 2 found a little difference between two structures, e.g. d(001) value of the core is 0·572 nm and that of the shell is 0·580 nm, corresponding to α and α' dimensions respectively. In addition, EDS analysis found a compositional disparity between the core and the shell. Figure 3 shows that the core contains only Si and N, while the shell contains Al, Y and O in addition to Si and

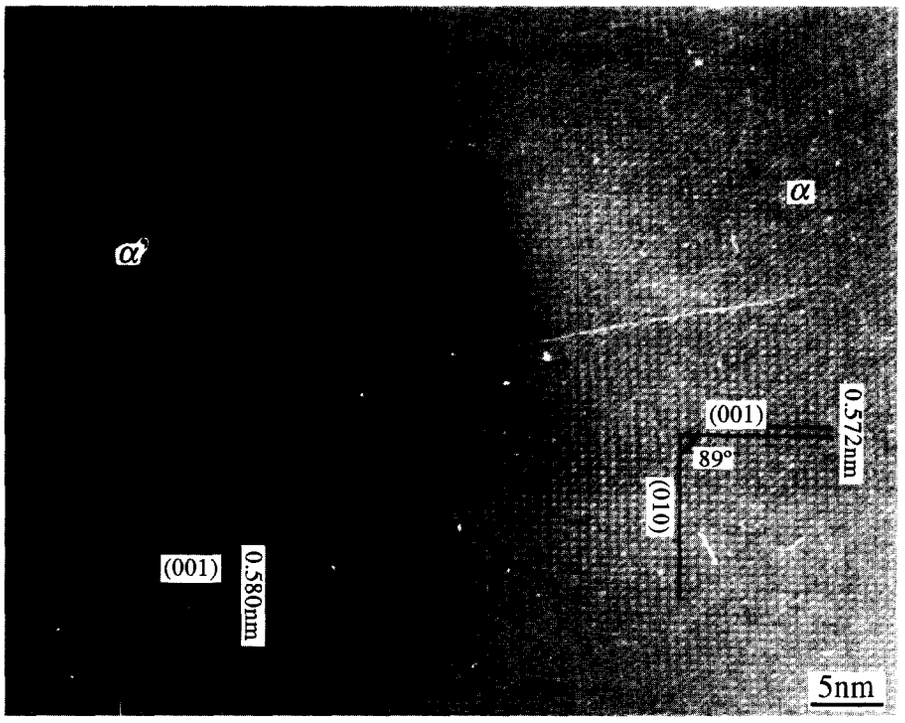

Fig. 2. HREM micrograph shows that the core and the shell have the same α-Si_3N_4 structure and the interface is coherent. Increased interplanar distances and structural deformation are discovered in both core and shell structures.

N. These results provide a ready explanation for the lighter contrast of the core, which lacks the strong, electron-scattering Y.[18] They also identify the core as α-Si_3N_4 and the shell as α'-SiAlON.

The d(001) values of α and α' structures measured in Fig. 2 are a little larger than the reported data ($c = 0{\cdot}562$ nm for α-Si_3N_4)[19] and the *in-situ* α' XRD result ($a = 0{\cdot}7817$ nm, $c = 0{\cdot}5696$ nm for α'-SiAlON). Moreover, SAD and HREM show that the crystal structure has changed from a rigid hexagonal symmetry in both α-Si_3N_4 core and elongated α'-SiAlON. Figure 4 shows the diffraction pattern of α' phase of [100] projection (a) and for comparison, also a pattern of the same projection but from an equiaxed grain (b). It can be seen in Fig. 4(a) that the *c* axis of the unit cell is no

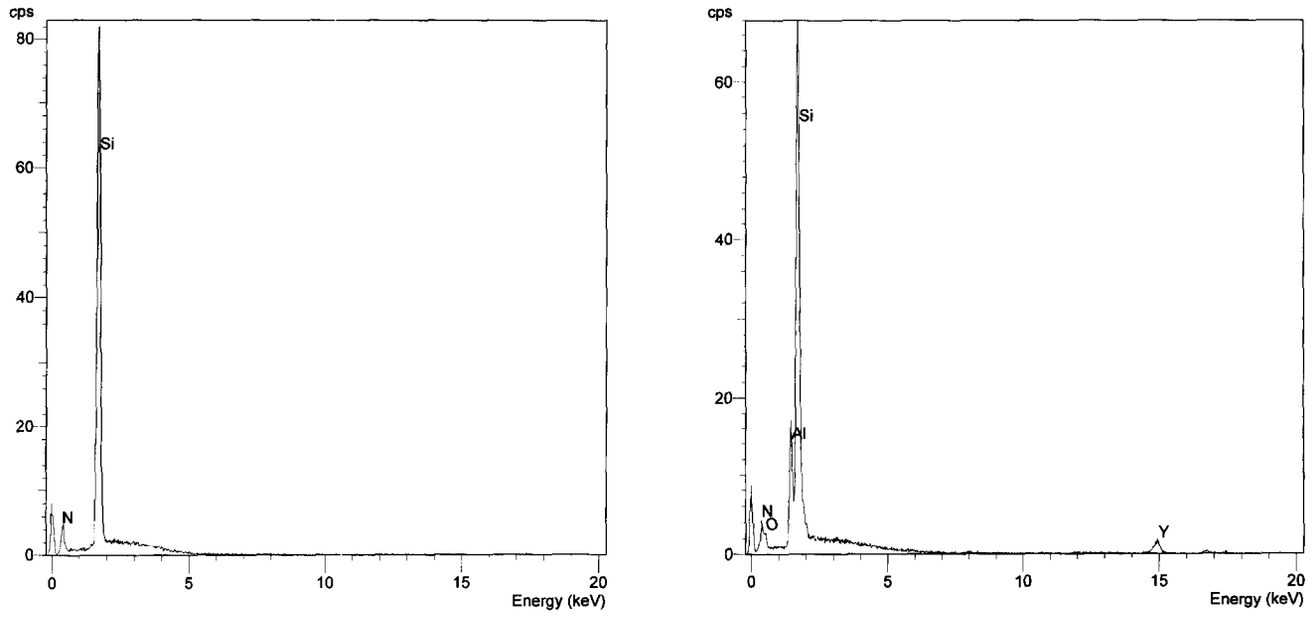

Fig. 3. EDS spectra taken from (a) the core and (b) the shell indicates α-Si_3N_4 and α'-SiAlON, respectively.

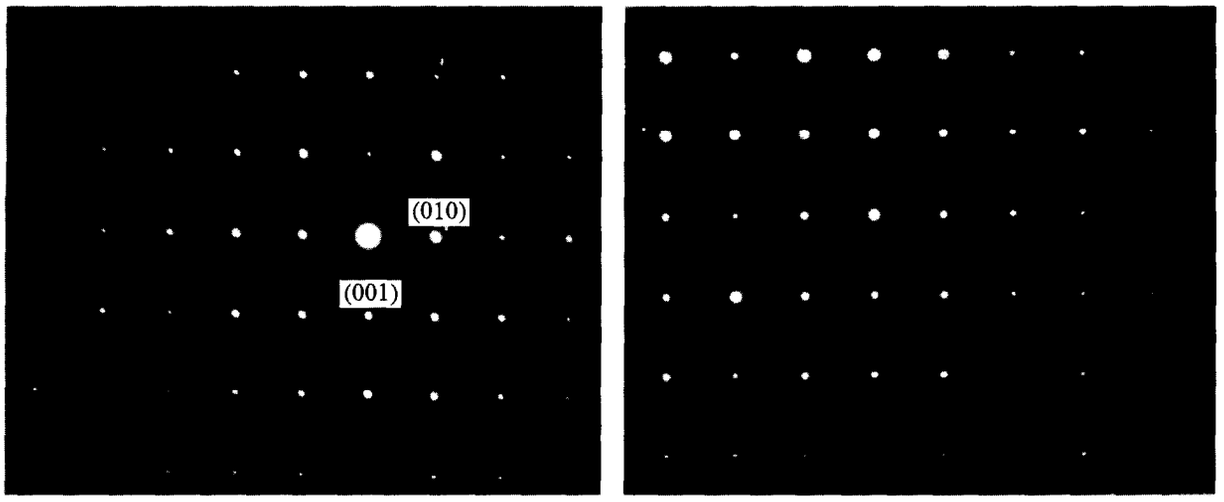

Fig. 4. [100] diffraction pattern of the elongated grain (a) showing (001) plane no longer normal to (010) plane. A pattern of [100] projection (b) from an equiaxed grain is also shown for comparison.

longer normal to the basal plane (001). It is tilted by an angle of no more than 2°. The lattice image in Fig. 2 has clearly shown such a distorted structure where the interplanar angle between (001) and (010) is about 89°. When we overlapped these two diffraction patterns, structural dilatation of the elongated α'-SiAlON was discovered (Fig. 5). Moreover, as has been indicated above, α-Si_3N_4 structure has dilated too. Both the lattice in core (α-Si_3N_4) and in shell (α'-SiAlON) have deformed indicating that the elongated grain had been formed from the precipitation onto a distorted α-Si_3N_4 core.

Another interesting discovery is the structural retrieval at the late stage of anisotropic growth. Figure 6 shows the diffraction pattern changes along the long axis of the elongated grain. Gradually weakened distortion and structural shrinkage was discovered along [001] direction from the core to the end of the rod where rigid hexagonal symmetry retrieved.

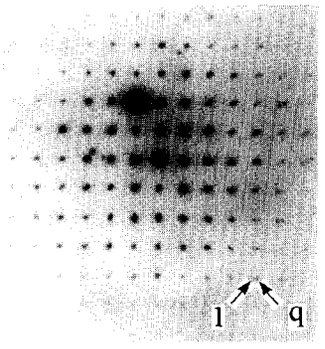

Fig. 5. A pattern resulting from overlapping two diffraction patterns shown in Fig. 4 illustrates that dilatation occurs for the structure of the elongated grain. 'l' represents dotts from elongated grain, whereas 'q' is from the equiaxed grain.

3.2 Growth process and grain morphology

TEM has confirmed an epitaxial growth mode operating in the growth process of the elongated α'-SiAlON after nucleation onto a deformed α-Si_3N_4 seed. Anisotropic coarsening indicated a higher growth rate in [001] direction.[8] In the present study, a structural defect was identified, produced due to faster precipitation in [001] direction. Figure 7(a) shows a stacking fault on the (001) plane caused by an extra inclusion of two layers with β'-SiAlON structure. While the SiAlON structure can be described as a stacking of Si(Al)-N(O) layers along the c axis in either an ABAB...

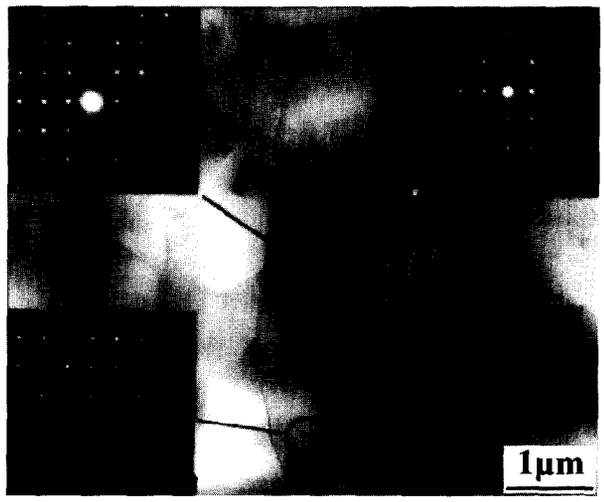

Fig. 6. Changes of diffraction patterns along the long axis of the elongated grain revealing weakened distortion and structural retrieval from the core to the end of the rod.

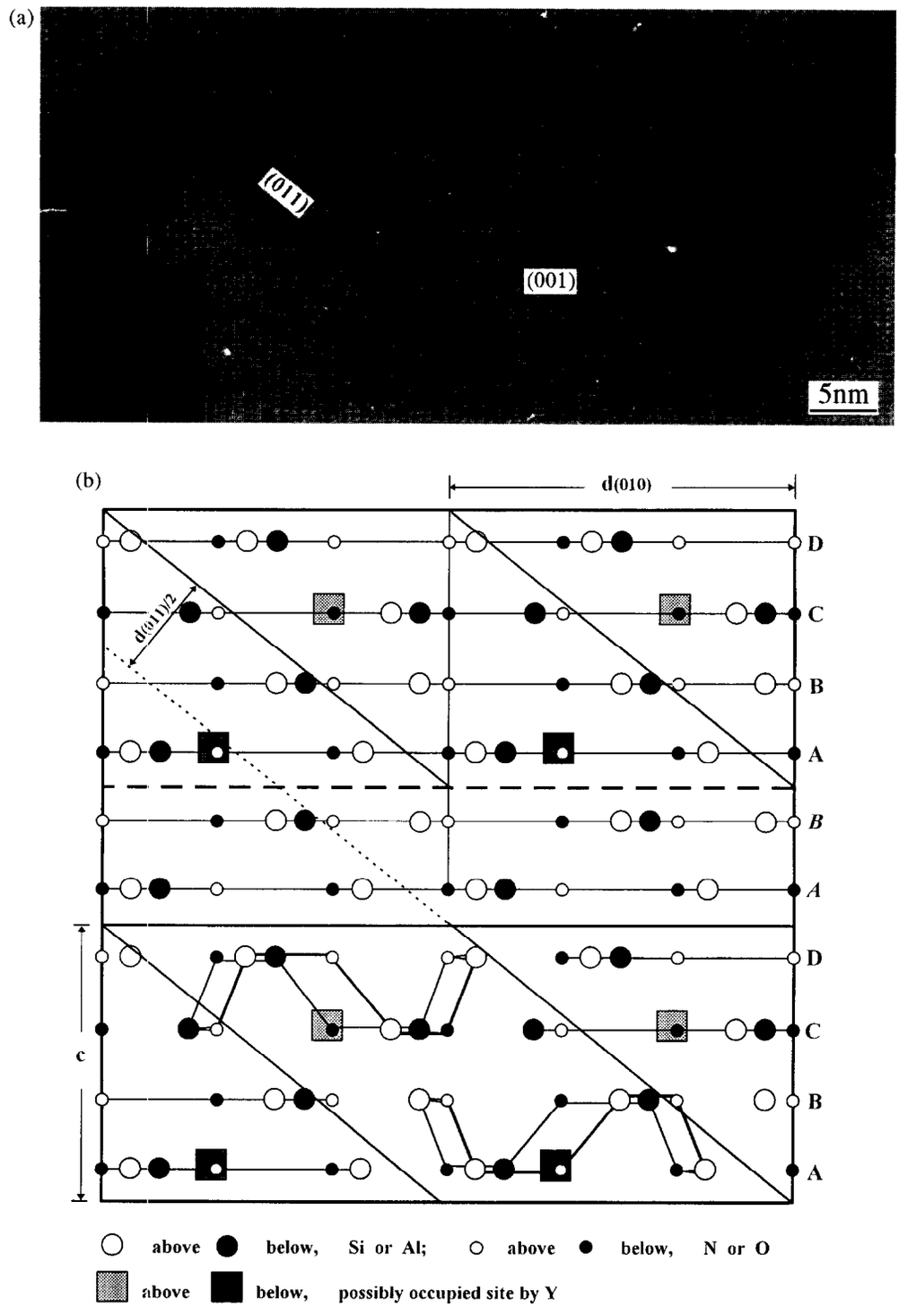

Fig. 7. Lattice image (a) showing an inclusion stacking fault on (001) plane and the atomic structural model (b) indicating an ABABCD sequence.

(β) or an ABCD... (α) sequence,[19] it is possible that the layers CD might be replaced by AB in the stacking sequences of atomic planes though it is not as ready to take place in SiAlON as in, for example, SiC. As to in-situ α' structural defect, an extra AB layer rather than CD layers stacked on the pre-existed AB layers, would result in an inclusion stacking fault with the stacking sequence as ABABCD. The atomic structural model in Fig. 7(b) gives a clear illustration of such a structural defect. It can be seen that (010) plane remains continuous across the stacking fault whereas (011) plane shifts half an interplanar distance. In addition, a lighter contrast within the stacking fault is further

evidence of the inclusion of β'-SiAlON structure which lacks Y atoms.

The grain morphology of the elongated α'-SiAlON grains is found to be different from those of β'-SiAlON. Though the majority of the side boundary remains sharp, a curved periphery, at least at some parts, is often found in elongated α'-SiAlON. The lattice image of the [210] front shown in Fig. 8 clearly illustrates a wavy boundary proceeding to the glass, the residual liquid phase. In addition, when the side boundary of the elongated grain attached to the small equiaxed grains at the grain growth stage, contact growth took place for the elongated grains; as can be seen in Fig. 6 the side boundary becomes concave. This coarsening character could never be found in β'-SiAlON materials.

4 Discussion

4.1 Formation mechanism of the elongated α'-SiALON grains

The TEM observations in the present study indicate that the precipitation process proceeds by heterogeneous nucleation of α'-SiAlON onto the remaining α-Si_3N_4 particles, followed by an epitaxial grain growth with a little lattice misfit at the α/α' boundary. Although the temperature was as high as 1825°C for the in-situ hot-pressing process, small amounts of oxynitride melted together with short densification time ($\sim$1 h) resulting in partial dissolution of some α-Si_3N_4 grains. The remaining α-Si_3N_4 grains with reduced particle size then act as the favoring sites for heterogeneous nucleation.

It has been considered that α'-SiAlON lacked any special growth direction, leading to equiaxed morphology. Previous work has rationalized this growth habit by chemical bonding considerations.[18] Recent work by Sun[20] and in-situ studies have found the presence of elongated α'-SiAlON grains growing along the [001] direction. Furthermore, our experimental results have revealed a feature of such elongated grain hitherto not reported in the literature.

The distortion of the structure discovered in both α-Si_3N_4 core and α'-SiAlON shell, whereas no change of the structure was found in equiaxed grains, suggests the strained structure be responsible for the anisotropic growth of α'-SiAlON. EDS analysis shows hardly any significant compositional difference between the elongated grain and the equiaxed grains. Thus, the influence possibly arising from compositional change can be excluded as a mechanism for the formation of the elongated grains.

We cannot give an accurate structure model of the deformed crystal due to the limitation of the operating conditions of our microscope. The experimental evidences suggests that the lattice strain must have changed the chemical bonding conditions especially on (001) plane, making it more favorable as the site for the fast deposition of atoms than other planes such as (010). The acicular cone in the [001] growth front (Fig. 1) indicates the presence of continuous growth steps characteristic of a diffuse interface, while along the [210] growth front, the interface is nearly flat due to the lack of growth sites. But wavy side boundary at some parts was more often found compared to those

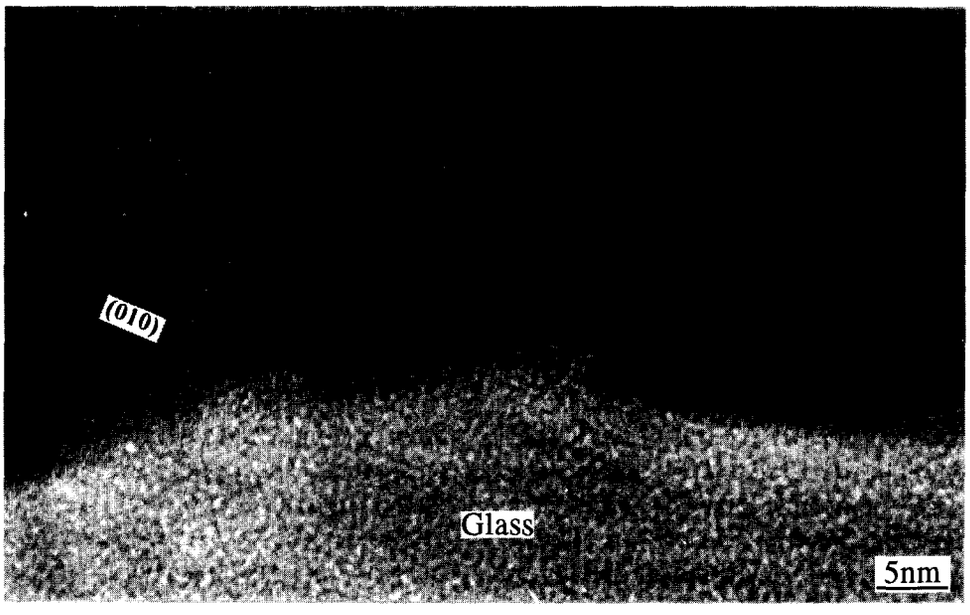

Fig. 8. HREM micrograph illustrating a wavy boundary at the [210] front.

elongated β′-SiAlON. This is a typical difference in appearance between α′ and β′ elongated grains.

Figure 5 demonstrates dilatation of the unit cell along both [001] and [210] directions. This dilatation loosened the atomic stacking and weakened the interatomic force. Such a change is more apparent on (001) plane, which can be confirmed by comparison of diffraction patterns in Fig. 5 where interplanar distance increases more for (010) plane than for (001) plane, i.e. atoms depart more on (001) plane. Moreover, tilting of the structure results in atomic rearrangement and modifies the bonding atmosphere, probably further favouring the atomic deposition on (001) plane. When atoms deposit on (001) face, as the strong bonds parallel to this face have weakened, layer growth, which takes effect in the growth process for equiaxed α′-SiAlON system, does not occur any more. Then the (001) face grows according to one-dimensional nucleation mechanism and the growth rate is fast, giving a stepped appearance.[21]

As the temperature was increased to as high as 1825°C, most starting powders were fully dissolved in the liquid. But some α-Si_3N_4 particles with reduced size remained undissolved. These particles were then the ideal sites for heterogeneous nucleation. Why the structure of α-Si_3N_4 seeds dilates is still uncertain. High temperature might have played a role in this situation. Homogeneity of composition excludes the influence possibly caused by compositional change. It is reported that tensile stress can cause strain-induced grain growth for superplastic ceramics.[22–25] It is then suggested that high temperature (dilatation) and high stress (strain) are responsible for the structural deformation of α-Si_3N_4 seeds, resulting in nucleation and anisotropic growth of α′-SiAlON. Whether the conditions of liquid phase, e.g. supersaturation, viscosity and eutectic temperature, might affect the formation of elongated grain needs further study.[26,27]

It may be concluded from the above discussion that high temperature, high sintering pressure and lower extra oxygen content in the starting powders and short sintering time for the retention of α-Si_3N_4 seeds, are the essential requirements for the formation of elongated α′-SiAlON. Therefore, lack of α-Si_3N_4 seeds at high temperature and critical formation conditions explain why elongated α′-SiAlON occurs much more rarely while elongated β′-SiAlON is a typical feature in any conventional preparation process.[26,28–30]

At the commencement of grain growth of the elongated crystal, the system is unstable due to the high strain energy. It might return to the stable state, i.e. rigid hexagonal structure immediately when its essential energy support disappears or hardly sustains any longer. TEM observations in Fig. 6 illustrated such trends back to the stable state in the sequence of grain growth. Gradually weakened distortion and structural shrinkage was found along [001] direction from the core to the end of the rod where rigid hexagonal symmetry retrieved, indicating the cessation of anisotropic growth. Consequently, the length of the elongated α′-SiAlON grains depends on the ability of the system to withstand the distortion of the structure.

4.2 Special growth habit and morphology

The discovery of an inclusion stacking fault on the (001) plane m the present TEM observation of the elongated grains confirms a high precipitation velocity in (001) direction. Even a small disturbance in the solution composition would produce structural defects. In addition, extra AB layers stacked on the pre-existing AB layers and resulted in ABAB stacking sequence, a typical feature of β′ structure. This is evidence that the structural defect might be a favorable site for the nucleation of α′ to β′ transformation. If the chemical environment permits, the β′ grain will surely be coarsened.

As has been mentioned above, the side boundary of the elongated α′-SiAlON grain often appears wavy. This special growth habit dominates the growth process probably because the strained structure has also modified, in some degree, the crystallochemical conditions at the (010) surface as indicated above, leading to an enhanced growth; i.e. increased growth sites and steps rather than one growth site with only one growth step sweeping over (010) surfaces in β′-SiAlON.[8] In fact, unlike the β′-SiAlON system where a high amount of liquid makes the small grains completely soluble and then material is transported to the large grains by diffusion, resulting in a progressive growth of the larger grains,[26,29,30] less glass in α′-SiAlON system makes the interaction of neighbouring grains easier to take place prior to the disappearance of small grains. When the growing front encounters the neighbouring grains, contact growth mode takes effect, indicating that new growth sites are readily produced. Further growth from the growth sites at intervals on (010) plane along the length direction gives a wavy morphology. As a whole, the deformation in structure not only changes the growth mode (anisotropic growth) but also modifies the grain morphology (wavy side boundary).

5 Conclusions

1. Both the structure of core (α-Si_3N_4) and shell (elongated α'-SiAlON) have dilated and deformed where c axis tilts by an angle of no more than 2°, suggesting changes of chemical bonding conditions especially on (001) plane resulting in anisotropic growth.
2. The elongated α'-SiAlON grains always contain an α-Si_3N_4 core, evidence that heterogeneous nucleation operates in the present system. The growth mode of the elongated α'-SiAlON on the deformed α-Si_3N_4 is epitaxial with misfit dislocations at the α/α' boundary.
3. High temperature, high pressure and rigid control of sintering time are the essential requirements for the formation of elongated grains.
4. Gradually weakened distortion and structural retrieval was discovered along [001] direction from the core to the end of the rod, suggesting the deformed structure be that of high energy and the length of the elongated α'-SiAlON grains depend on the ability of the system to withstand the distortion of the structure.
5. A wavy side surface rather than a flat facet was found for elongated α'-SiAlON indicating an enhanced growth, i.e. increased growth sites and steps, correlative to the changes of chemical bonding conditions at this surface due to the deformation of the structure.
6. An inclusion stacking fault was identified with the stacking sequence ABABCD, the result of fast precipitation on (001) plane. It is suggested that the structural defect might be a favorable site for the nucleation of α' to β' transformation.

References

1. Hwang, Z.-K., Tien, T.-Y. and Yen, T.-S., Subsolidus phase relationships in Si_3N_4–AlN–rare-earth oxide systems. *Journal of Am. Ceram. Soc.*, 1986, **69**, C-241–C-242.
2. Hwang, Z.-K., Greil, P. and Petzow, G., Formation of α-Si_3N_4 solid solutions in the system Si_3N_4–AlN–Y_2O_3. *Journal of Am. Ceram. Soc.*, 1983, **66**, C-96–C-97.
3. Ekstrom, T. and Nygren, M., SiAlON ceramics. *Journal of Am. Ceram. Soc.*, 1992, **75**, 259–276.
4. Cao, G. Z. and Metselaar, R., α'-SiAlON ceramics: A review. *Chem. Mater.*, 1991, **3**, 242–252.
5. Ekstrom, T., Preparation and properties of α-Si-Al-O-N ceramics. *Journal of Hard Mater.*, 1992, **3**, 109–118.
6. Ekstrom, T. and Persson, J., Hot-hardness behaviour of yttrium SiAlON ceramics. *Journal of Am. Ceram. Soc.*, 1990, **73**, 2834–2838.
7. Ekstrom, T., Effect of composition, phase content and microstructure on the performance of yttrium Si-Al-O-N ceramics. *Mater. Sci. Eng.*, 1989, **A109**, 341–349.
8. Hwang, C. M., Tien, T. Y. and Chen, I-W., Anisotropic grain growth during final stage sintering of silicon nitride ceramics. In *Sintering '87* ed. S. Somiya, M. Shimada, M. Yoshimura and R. Watanabe. Elsevier Applied Science, New York, 1988, pp. 1034–1039.
9. Wotting, G., Kanka, B. and Ziegler, G., Microstructural development, microstructural characterization and relation to mechanical properties of dense silicon nitride. In *Non-Oxide Technical and Engineering Ceramics*, ed. S. Hampshire. Elsevier Applied Science, London, UK, 1986, pp. 83–96.
10. Chetfield, C., Ekstrom, T. and Mikus, M., Microstructural investigation of alpha-beta yttrium SiAlON materials. *Journal of Mater. Sci.*, 1986, **21**, 2297–2307.
11. Evans, A. G. and Sharp, J. V., Transmission electron microscopy of silicon nitride. In *Electron Microscopy and Structure of Materials*, ed. G. Thomas, R. M. Fulruth and R. M. Fisher. California Press, Berkeley, CA, 1972, pp. 1141–1153.
12. Kossowsky, R., The microstructure of hot-pressed silicon nitride. *Journal of Mater. Sci.*, 1973, **8**, 1603–1615.
13. Evans, A. G. and Sharp, J. V., Microstructural studies on silicon nitride. *Journal of Mater. Sci.*, 1971, **6**, 1292–1302.
14. Nordberg, L.-O., Ekstrom, T., Svensson, G. and Wen, S. L., Hot-pressed SiC-whisker reinforced α-SiAlON composites. *Journal of Hard Mater.*, 1993, **4**, 121–135.
15. Ekstrom, T. and Olsson, P. O., β SiAlON ceramics with TiN-particle inclusion. *Journal of Europ. Ceram. Soc.*, 1994, **13**, 551–559.
16. Petrovic, J. J. and Honell, R. E., $MoSi_2$ particle reinforced SiC and Si_3N_4 matrix composites. *Journal of Mater. Sci. Lett.*, 1990, **9**, 1083–1084.
17. Kao, M., Properties of silicon nitride-molybdenum disilicide particulate ceramic composites. *Journal of Am. Ceram. Soc.*, 1993, **76**, 2879–2883.
18. Hwang, S. L. and Chen, I-W., Nucleation and growth of α'-SiAlON on α-Si_3N_4. *Journal of Am. Ceram. Soc.*, 1994, **77**, 1711–1718.
19. Hampshire, S., Park, H. K. and Thompson, D. P., α'-SiAlON ceramics. *Nature (London)*, 1978, **274**, 880–882.
20. Unpublished work by Prof. Sun, W.Y. in Shanghai Institute of Ceramics, China.
21. Hartman, P., Structure and morphology. In *Crystal Growth: An Introduction*, ed. P. Hartman. North-Holland, Amsterdam, Holland, 1973, pp. 367–402.
22. Wu, X. and Chen, I-W., Exaggerated texture and grain growth in a superplastic SiAlON. *Journal of Am. Ceram. Soc.*, 1992, **75**, 2733–2741.
23. Wilkinson, D. S. and Caceres, C. H., On the mechanism of strain-enhanced grain growth during superplastic deformation. *Acta Metall.*, 1984, **32**, 1335–1345.
24. Wang, J.-G. and Raj, R., Mechanism of superplastic flow in a fine-grained ceramic containing some liquid phase. *Journal of Am. Ceram. Soc.*, 1984, **67**, 399–409.
25. Chen, I-W. and Xue, L. A., Development of superplastic structural ceramics. *Journal of Am. Ceram. Soc.*, 1990, **73**, 2585–2609.
26. Hwang, S. L. and Chen, I-W. Nucleation and growth of β-SiAlON. *Journal of Am. Ceram. Soc.*, 1994, **77**, 1719–1728.
27. Gazza, G. E., Effect of yttria additions on hot-pressed Si_3N_4. *Am. Ceram. Soc. Bull.*, 1975, **54**, 778–781.
28. German, R. M., Farooq, S. and Kipphut, C. M., Kinetics of liquid phase sintering. *Materials Science and Engineering*, 1988, **A105/106**, 215–224.
29. Lee, F. and Bowman, K. J., Texture and anisotropy in silicon nitride. *Journal of Am. Ceram. Soc.*, 1992, **75**, 1748–1755.
30. Lee, D. D., Kang, S. L. and Yoon, D. N., Mechanism of grain growth and α'-β' transformation during liquid-phase sintering of β'-SiAlON. *Journal of Am. Ceram. Soc.*, 1988, **71**, 803–806.